GA–A23817

# ELMs AND THE ROLE OF CURRENT-DRIVEN INSTABILITIES IN THE PEDESTAL

by
P.B. SNYDER and H.R. WILSON

NOVEMBER 2001

## DISCLAIMER

GA–A23817

# ELMs AND THE ROLE OF CURRENT-DRIVEN INSTABILITIES IN THE PEDESTAL

by
P.B. SNYDER and H.R. WILSON*

This is a preprint of a paper to be presented at the 8th International Workshop on Plasma Edge Theory in Fusion Devices in Espoo, Finland, September 10–12, 2001 and to be published in the *Proceedings.*

*EURATOM/UKAEA Fusion Association, Culham, Abingdon, United Kingdom.

Work supported by
the U.S. Department of Energy under
Grant No. DE-FG03-95ER54309 and the United Kingdom
Department of Trade and Industry and EURATOM

GENERAL ATOMICS PROJECT 03726
NOVEMBER 2001

## ABSTRACT

Edge localized modes (ELMs) can limit tokamak performance both directly, via large transient heat loads to divertor plates, and indirectly, through constraints placed on the edge pedestal height which impact global confinement. Understanding the physics of ELMs has proved challenging, in part because the sharp edge pressure gradients and consequent large bootstrap currents in the pedestal provide drive for a variety of magnetohydrodynamic (MHD) instabilities over a wide range of toroidal mode numbers ($n$). We present a brief review of recent developments in ELM theory, focusing on ELMs whose frequency increases with input power, and emphasizing theories which incorporate current-driven MHD instabilities such as external kink or "peeling" modes. We describe recent progress both in analytic theory of peeling-ballooning modes, and in the development of computational tools which can calculate edge MHD growth rates in shaped toroidal geometry over the full relevant spectrum of $n$. This progress has led to the development and refinement of ELM theories based on peeling-ballooning modes, including models for ELM characteristics and temperature pedestal limits. Comparisons of ELM theory with experiment, and recent experimental efforts to control ELMs will also be discussed.

## 1 Introduction

The high confinement regime known as H-mode is a promising operational regime for a tokamak fusion device. However, steady state operation in H-mode is generally accompanied by the bursty edge perturbations known as edge localized modes (ELMs). ELMs have the beneficial effect of transporting density and impurities across the H-mode edge transport barrier ("pedestal") region, however, large ELMs can produce high peak heat loads on the divertor plates which may be intolerable in a fusion reactor. Perhaps even more important, ELMs limit the pedestal pressure gradient, and, together with edge transport, can limit the pressure and temperature at the top of the pedestal (i.e. the "pedestal height"). Both theory-based transport models and experimental observation indicate a strong dependence of the overall confinement in the core of a magnetic fusion device on the pedestal height. Achieving at least a modestly high pedestal appears necessary for successful operation of currently envisioned Next Step devices, and determining under what conditions a high pedestal may be achieved in conjunction with tolerable ELMs requires a detailed, predictive understanding of ELM physics.

The theory of ELMs has been an active area of investigation over the past decade, and several comprehensive reviews of both ELM [1, 2, 3, 4] and pedestal [5, 6] theory and experimental results are available. In this paper, we focus primarily on following a research thread that has explored the impact of the pedestal current, both in driving edge kink or "peeling" instabilities and in lowering edge shear and opening access to the second stability regime for ballooning modes. The sharp pressure gradients found in the H-mode transport barrier can drive a strong, collisionality dependent bootstrap current in the pedestal which can significantly alter pedestal stability properties, and has proven to be fertile ground for developing ELM theories which predict a number of ELM and pedestal characteristics observed in experiments. Recent progress in both analytic and numerical studies of peeling and coupled peeling-ballooning modes will be summarized, including developing models for ELMs and pedestal characteristics, and comparisons with experiment.

Section 2 gives a brief discussion of ELM phenomenology and categorization, and Section 3 discusses theoretical models of ELMs which incorporate the impact of pedestal current. Linear ideal MHD-based theories are discussed first, initially in analytic limits and simple geometry to gain physical insight on peeling modes, second stability, and peeling-ballooning coupling, and then in shaped toroidal geometry. Extensions to the ideal MHD model, primarily involving the inclusion of diamagnetic stabilization, are discussed in Section , and nonlinear simulations and transport codes including ELM models in Section . A brief summary is found in Section 4.

## 2 Phenomenology

ELMs are short, repetitive perturbations of plasma in the edge region, which occur during H-mode and VH-mode operation and lead to particle and energy loss. A rich variety of ELM phenomena have been observed, and are well described in recent reviews by Suttrop [3] and Zohm [1].

ELMs are typically categorized into types I, II, and III, following a scheme introduced in Ref. [7]. Type I ELMs are characterized by a repetition frequency that increases with input power. Usually type I ELMs appear as sharp, well isolated bursts, which can be quite large ("giant ELMs"), though small type I ELMs are also observed. In contrast type III ELMs have a repetition frequency that decreases with input power, and tend to occur at heating powers close to the H-mode power threshold. Type III ELMs tend to have relatively high repetition frequency and small power loss per ELM.

During the quiescent phase of the ELM cycle, the pressure gradient in the pedestal region typically increases (or first increases and then stays relatively constant for a time) before an ELM event is triggered. The pressure gradient immediately prior to an ELM is often characterized relative to the ideal MHD ballooning stability limit.[1] Type I ELMs generally occur at or above the ideal ballooning limit, while type III ELMs usually occur well below it. Magnetic fluctuations are associated with both type I and type III ELMs. Type III ELMs are typically observed to have a coherent magnetic precursor with toroidal mode number $n \sim 6$–$15$. Type I ELMs are typically observed either without magnetic precursors, or with intermediate $n \sim 3$–$10$ precursors, though lower $n \sim 1$–$2$ precursors have been observed in some cases. On most tokamaks it is difficult to clearly measure fluctuations of higher mode number ($n > 10$).

Type II ELMs have a frequency which increases with power and occur at pressure gradients near the ideal ballooning limit, but have high frequencies and small sizes typical of type III rather than type I ELMs. Because type II ELMs are difficult to distinguish from small type I ELMs, we will generally consider them together.

Likely quite closely related to ELMs are the "outer modes" which have been observed to degrade plasma performance in JET [8]. Outer modes cause a slow and steady increase in the edge $D_\alpha$ signal, in contrast to the bursty signal characteristic of ELMs. Outer modes are localized around and outside the $q = 3$ surface and typically have $n = 1$. Other H-mode edge quasi-steady state regimes have recently been identified including the "enhanced $D_\alpha$" (EDA) regime on Alcator C-Mod [9, 10], and the quiescent H-mode on DIII-D [11].

[1] Note that in practice, a "nominal ballooning limit" is often used for this purpose, due to the difficulties of accurately reconstructing pedestal equilibria, and in some cases because of the absence of a true ballooning limit when the pedestal is in the second regime of stability to ballooning modes. (See later sections for more discussion of second stability.) This nominal ballooning limit is usually calculated either by extrapolating the core ballooning limit into the pedestal, or by calculating the ballooning limit in the pedestal assuming zero edge current.

Here we focus primarily on both large and small type I/type II ELMs, as these occur in the high pedestal pressure regimes of interest to next step devices, and provide *de facto* limits on the pedestal height achievable in experiments.

# 3 Theoretical Analysis of ELMs

## 3.1 Ideal MHD

The magnetic fluctuation signatures, proximity to the ideal ballooning limit, and short timescale for ELM growth suggest a relationship between ELMs and ideal MHD instabilities that has been explored by many authors.

However, a simple model based entirely on pressure driven high-$n$ ideal ballooning modes, without consideration of the edge current, appears to be ruled out by experiment. While the high-$n$ ideal ballooning limit does correspond well to the observed type I ELM threshold in many regimes, recent experiments with high edge spatial resolution diagnostics indicate that the ideal ballooning limit can be substantially exceeded, and that observed pressure gradient limits do not always scale as expected from ideal ballooning theory [12, 13]. Figure 1 shows the results from a scan of the plasma triangularity in DIII-D, indicating both that the ideal ballooning limit can be substantially exceeded at high triangularity, and that the strong scaling of the pressure gradient limit with triangularity is not predicted by ideal ballooning theory [12]. Similar scaling of normalized pressure gradient with triangularity has been observed on JT-60U and ASDEX-U.

Incorporating the impact of edge current and finite $n$ appears to have the potential to overcome the above difficulties and lead to more comprehensive and accurate theories of ELM stability. The sharp pressure gradients in the H-mode pedestal can drive strong bootstrap currents which dramatically impact edge MHD stability. Edge current plays a complex dual role in the stability picture. On the one hand, edge current provides a source of free energy which drives external kink or "peeling" modes in the edge. On the other hand, edge current reduces the magnetic shear ($\hat{s}$) in the edge, which can open up a window of second stability to high-$n$ ballooning modes, and increase the pressure gradient threshold.

Recent investigations of pedestal MHD theory have focussed on the edge current, and the kink/peeling modes it drives, as well the ballooning modes it can stabilize. Coupling between peeling and ballooning modes has been studied both analytically and numerically and new tools have been developed to accurately treat the wide range of $n$ numbers which can potentially be unstable in the pedestal.

### 3.1.1 Current Driven Modes

In the presence of finite edge current, external modes localized near the plasma edge can be driven unstable. These modes were dubbed "peeling" modes by Frieman *et al* [14], and localized criteria for peeling stability have been given by Lortz [15], Wesson [16], and Connor *et al.* [17]. Peeling modes are found to be most unstable when a rational surface is located just outside the plasma, minimizing the stabilizing influence of magnetic perturbations in the vacuum. In this limit, for large mode

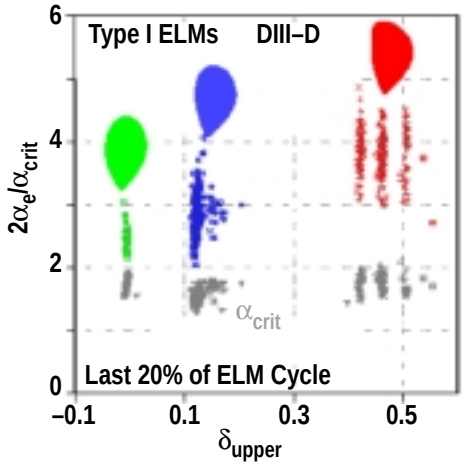


Fig. 1: Normalized edge pressure gradient ($\alpha$) averaged over the last 20% of the ELM cycle as a function of the upper triangularity of the plasma shape. Also plotted is the critical normalized pressure gradient for ideal ballooning stability ($\alpha_{CRIT}$), calculated in the absence of edge $J_{bs}$.

number, a necessary stability criterion for peeling modes can be written [17]:

$$\sqrt{1-4D_M} > 1 + \frac{2}{2\pi q'} \oint \frac{J_\parallel B}{R^2 B_p^3} dl \quad , \tag{1}$$

where $D_M$ is the Mercier coefficient, $J_\parallel$ is the current density along the magnetic field $\mathbf{B}$, $q'$ is the derivative of the safety factor with respect to the poloidal flux $\Psi$, $B_p$ is the poloidal field, and $dl$ is the poloidal arc length element, with all quantities evaluated at the plasma surface. Finite (positive) edge current is clearly destabilizing, while magnetic shear is stabilizing, and the pressure gradient is also stabilizing, as it increases $D_M$. Equation (1) provides useful insight into peeling mode stability, however it is a necessary, but not sufficient condition for peeling stability, as it considers only modes which are radially localized on the scale of the distance between rational surfaces, and it neglects the stabilizing contribution of the vacuum energy. At finite mode number, particularly for low $n$ modes in shaped geometry, multiple poloidal harmonics couple and a more detailed treatment is required to calculate stability thresholds.

### 3.1.2 Second Stability and Peeling-Ballooning Coupling

Studies focusing on the higher end of the $n$ spectrum have emphasized the impact of second stability to ballooning modes, and of coupling of peeling and ballooning modes that occurs at finite $n$. Analytic and numerical calculations in simplified geometry have shed light on the underlying physics.

Hegna *et al* [18] studied the coupling between current driven peeling and pressure driven ballooning modes, and cast the ideal energy functional $\delta W$ in a form that clearly demonstrates the destabilizing nature of the interaction between peeling and ballooning modes at finite-$n$. Connor *et al* [17] developed an extension of the ballooning transformation, which includes surface terms needed to treat peeling-ballooning modes.

A number of papers [17, 19, 20, 21, 22] have employed this formalism to develop a coherent picture of the complex role of peeling-ballooning coupling and its relationship to second stability in the edge.

Figure 2 [19] illustrates several important features of peeling-ballooning coupling via stability calculations in $s-\alpha$ geometry, with the addition of a "magnetic well factor" $d_m = D_M s^2/\alpha$ which models the effects of shaping and finite aspect ratio. In the $n \to \infty$ limit, the peeling and ballooning thresholds can both be obtained from simple 1D calculations [17], and these are shown as the "pure peeling" and "pure ballooning" curves in Fig. 2(a). Note that the peeling mode is driven unstable by edge current [$s = 2(1 - J_a/\langle J \rangle)$, where $J_a$ is the current density on the outermost flux surface, and $\langle J \rangle$ is the average current density in the plasma] and stabilized by finite alpha as expected [Eq. (1)], and that a wide stable path to the second stable region exists, between the pure peeling and pure ballooning unstable regions. However, at finite values of $n$ ($n = 20$), the peeling and ballooning modes couple and can close off access to the second stability region, as shown by the "2-D coupled mode" curves in Fig. 2(a). Increasing the magnetic well decouples the modes and reopens second stability access as shown in Fig. 2(b). The strength of the peeling-ballooning coupling is also a function of $n$, as illustrated in Fig. 3(a) [21], and the second stability gap opens more easily for higher $n$ modes. As the magnetic well deepens (i.e. shaping improves), the edge stability transitions rapidly from a regime in which essentially no $n$'s have second access ($n \gtrsim 50$ will generally be FLR stabilized), to a regime in which all $n \gtrsim 10$ have access to second stability.

Hegna *et al* [18] and Connor *et al* [17] have used stability diagrams in $J_a$, $p'_a$ space (in the absence of second stability access) to construct a model for ELMs. Type I ELMs are proposed to occur when the pedestal is heated to the ballooning limit ($p' = p'_c$), where it sits until the edge current increases to the point where it becomes peeling unstable, and then an ELM is triggered, dropping both $j_a$ and $p'$ back to stable levels before the cycle repeats. Type III ELMs are hypothesized to result from trajectories encountering the peeling limit at $p' < p'_c$.

Ramos *et al* [23] have recently derived a necessary stability criterion for high-$n$, edge-localized peeling and ballooning modes that requires only one dimensional calculations, effectively extending the conventional high-$n$ ballooning formulation to include peeling modes. This formulation is applicable for arbitrary $q_a$ (i.e. not just in the limit where the nearest vacuum rational surface approaches the plasma-vacuum boundary), and in principle can be used for arbitrary cross section shape. High-$n$ peeling mode stability calculations using this formulation have been successfully carried out in $s-\alpha$ geometry.

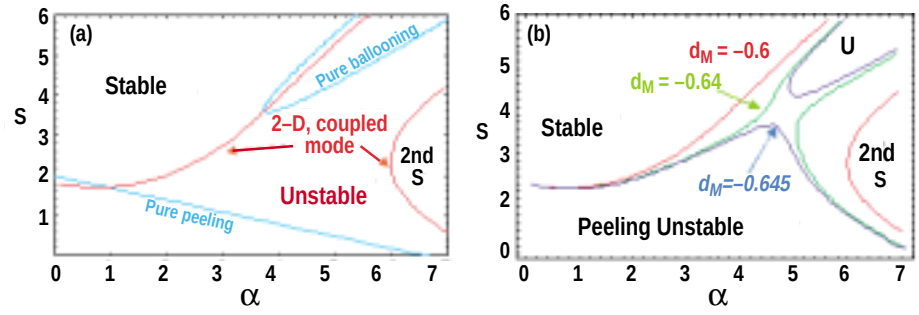


Fig. 2: The marginal stability contours in $s-\alpha$ space for a) the $n=\infty$ pure peeling and pure ballooning modes, as well as the $n=20$, $d_m=-0.6$ 2-D coupled peeling ballooning mode and b) a sequence of curves for the $n=20$ 2-D coupled mode, with $d_m=-0.6,-0.64,-0.645$, showing second stability access reopening at the deepest well ($d_m=-0.645$).

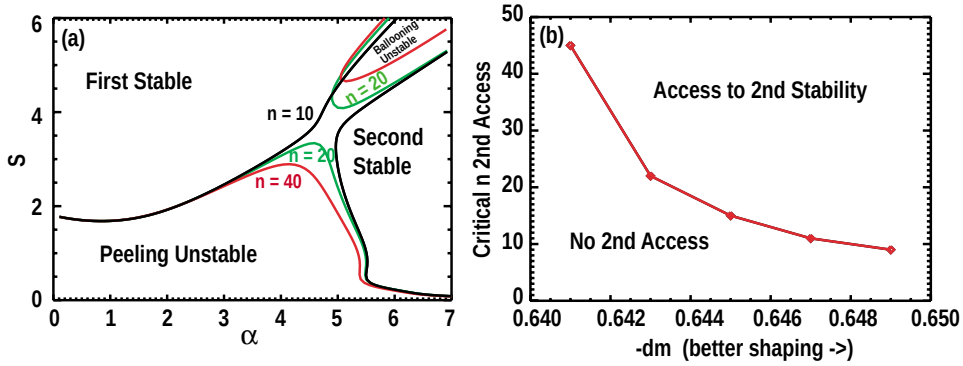


Fig. 3: (a) Marginal stability contours in $s-\alpha$ for the 2D coupled peeling-ballooning mode at $n=10,20,40$, $d_m=-0.645$, (b) Calculated marginal value of $n$ for second stability access as a functions of the magnetic well $d_m$.

### 3.1.3 Peeling Mode Stability in Tokamak Geometry

While analytic and simplified geometry calculations are useful for gaining physical insight, detailed stability calculation in real tokamak geometry is needed to fully develop MHD-based ELM models and make quantitative comparisons to experiment. Recent improvements in numerical tools and computing power have allowed steadily more detailed MHD stability calculations, incorporating the whole confined plasma approaching, or even reaching, the separatrix, and treating the full relevant spectrum of $n$ values at high resolution.

It was first proposed in Turnbull *et al* [24] that ELMs are essentially ideal kink modes (i.e. peeling modes) localized near the edge and driven by a combination of $p'$ and $j$. In kink/ballooning stability optimization studies of circular H-mode plasmas, it was found that the zero $\beta$ current-driven surface mode is destabilized by finite $p'$ when the pedestal current profile is broad, driving both $n=1$ and higher $n$ modes unstable. An ELM cycle model was proposed in which the broadening of the current profile

following the L-H transition drives the first ELM, after which the plasma relaxes into a higher shear, lower current state, and the process repeats as the current builds up.

Manickam [25] performed a detailed numerical study of $n = 1$ peeling mode[2] stability in circular and shaped toroidal geometry, and proposed an ELM model based on the role of edge current in driving $n = 1$ ideal modes. Manickam found that $n = 1$ mode stability is determined by a combination of edge safety factor $q_a$ (in particular, the proximity of the nearest vacuum rational surface to the plasma is quite important), current density at the plasma edge $J_a/J_{axis}$, the current density in the outer 10% of the plasma $I(90)$, and plasma $\beta$, the ratio of plasma pressure to magnetic pressure. Magnetic shear is the principle stabilizing mechanism, and edge current is strongly destabilizing. Manickam notes that at finite $\beta$, the $n = 1$ modes can have relatively broad radial extent, coupling to several poloidal harmonics, and may have an anti-ballooning nature, with the mode amplitude peaked on the high field side. The ELM model proposed involves a cycle in which edge current builds up, exceeds a threshold and triggers an $n = 1$ mode, which may be either strongly localized (small ELM) or coupled to interior harmonics (giant ELM), depending on conditions. The ELM ejects current, and the cycle repeats, with the period depending on plasma transport properties near the edge. This ELM model predicts ELMs with $n = 1$, multiple poloidal harmonics, and Alfvénic growth times, with mode structures that may peak either on the high or low field side. Manickam suggests edge current drive as a possible means for controlling these ELMs.

Huysmans *et al* [26] studied the influence of edge current and pressure gradient on low $n = 1$–4 peeling modes in both circular and JET-like plasma shapes. As expected, the edge current is destabilizing to low-$n$ modes. The pressure gradient ($p'$) is found to be stabilizing at small values, well below the ideal ballooning limit ($p'_c$), with the stabilizing effect strongest for the lowest $n$. As $p'$ approaches the ballooning limit, $p'$ becomes destabilizing for $n > 1$ modes, with the $n = 4$ mode (the largest $n$ value studied) becoming the most unstable for $p'$ well above $p'_c$. The edge bootstrap current from transport simulations of JET hot ion H-modes is found to be sufficient to drive peeling modes. At low values of $\beta_p$ and triangularity ($\delta$), there is no access to 2nd stability, as peeling modes become unstable before the edge becomes second stable, while for larger $\beta_p$ and $\delta$ access to second stability opens at much smaller values of the edge current, below the low $n$ peeling mode threshold.

More recently Huysmans *et al* [27, 28] have employed the efficient MISHKA1 [29] incompressible ideal MHD eigenvalue code to study peeling modes in JET. Outer modes in JET have been convincingly identified as $n = 1$, $m \sim 4$–6 peeling (i.e.

[2]Manickam refers to these modes as external kinks, noting that when edge safety factor $q_a$ is near a rational surface the mode has a strong edge localized peeling structure, while for $q_a$ further from a rational surface, the instability has a broader radial structure incorporating several poloidal harmonics. For simplicity of terminology, we will refer to all edge region current driven instabilities as peeling modes, regardless of whether they are dominated by a single poloidal harmonic.

external kink) modes via comparison of experimental trajectories to computed stability boundaries, and detailed comparisons between soft X-ray amplitude and phase data, and predictions from MISHKA1 [27]. Figure 4 [27, 8], shows the results of a current ramp down experiment in JET. Without current ramp down (solid line), the outer mode goes unstable near $t = 13s$, approximately when the discharge is computed to cross the $n = 1$ peeling stability boundary. However, when the current is ramped down (dashed line), the $n = 1$ peeling stability boundary is not crossed, and a giant ELM, rather than an outer mode, occurs first at $t \sim 13.5s$.

Wilson [22] and Snyder [21, 30] have developed the ELITE stability code to efficiently treat intermediate to high-$n$, $5 < n < 50$ instabilities in toroidal geometry with arbitrary cross section. ELITE employs an expansion of the variational energy in $1/n$, retaining the first two orders. ELITE also employs an expansion in poloidal harmonics ($m$), and takes advantage of the fact that, while very large numbers of poloidal harmonics must be retained for high $n$ computations, field line bending tends to localize each $m$ near its rational surface, such that only a small number of $m$'s are needed at each radial position. ELITE has been successfully benchmarked against MISHKA1 for $4 < n < 50$ [22], and used to study pedestal stability and develop ELM and pedestal models. Figure 5 [22] shows the stability boundary calculated from ELITE for the range $5 < n < 31$, employing JET-like equilibria with elongation $\kappa = 1.6$, triangularity $\delta = 0.5$, and a fixed pressure profile shape. For these equilibria, second stability access is possible at high $n$, but intermediate $n \sim 6$–$8$ modes close off second stability access. The radial mode structures of the limiting modes in each regime is also shown, and it is suggested that the narrow peeling modes at high $J$, low $\beta_N$ lead to small ELMs, while the wide $n = 6$–$8$ peeling-ballooning modes that occur at high $J$ and high $\beta_N$ lead to large ELMs. Because the current profile (Ohmic + collisional bootstrap) is calculated self-consistently with the given temperature and density profiles, and because there is a monotonic relationship between temperature and the resulting current at fixed pressure (largely because the collisional bootstrap current increases strongly when density is lowered and temperature increased), it is possible to recast Fig. 5 as a stability boundary in $T_{ped}$, $\beta_N$ space, and therefore to directly calculate the MHD stability imposed limits on $T_{ped}$. Such a calculation is shown in Fig. 6 for two values of the triangularity, $\delta = 0.3$ and $\delta = 0.5$, showing that higher $T_{ped}$ can be reached at higher triangularity. It should be noted that in such diagrams, the $T_{ped}$ stability limit is a "soft" limit, in that it may be crossed temporarily, but an instability will be triggered once the bootstrap current rises to its steady state value.

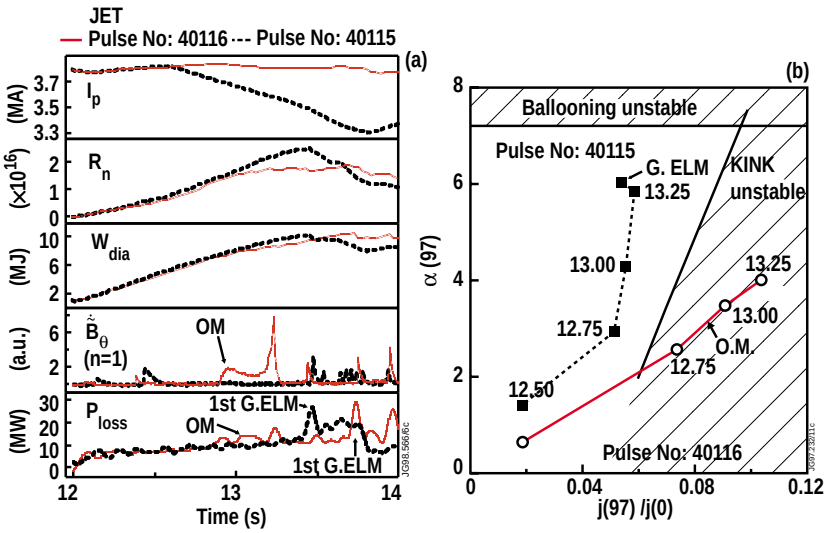


Fig. 4: Comparison of temporal evolution and trajectories in $\alpha$,$J$ (at 97% of the enclosed poloidal flux) space of two similar JET hot-ion H-mode discharges with and without current ramp-down. The experimental trajectories are compared with computed stability boundaries for the high $n$ ballooning and $n = 1$ peeling modes.

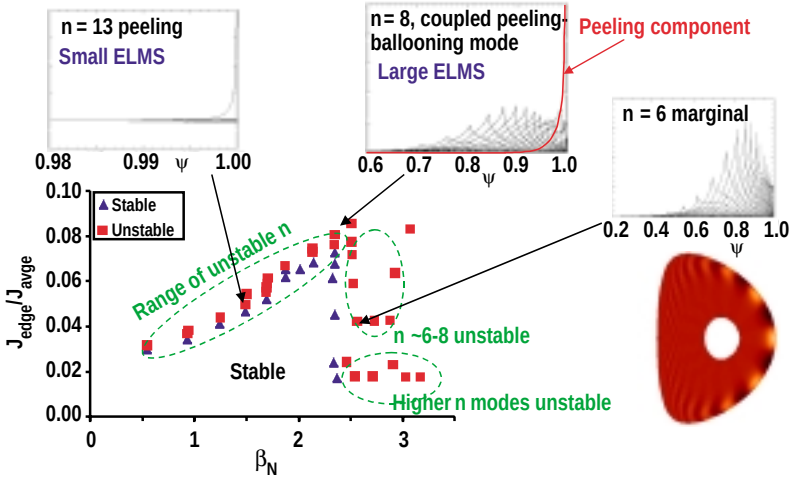


Fig. 5: Stability boundary in $J$, $\beta_N$ space for the range $5 < n < 31$ for JET-like equilibria with $\kappa = 1.6$, $\delta = 0.5$. The radial mode structure of the limiting instability in different regimes is also shown, along with a contour plot of the 2D structure of an $n = 6$ peeling-ballooning mode.

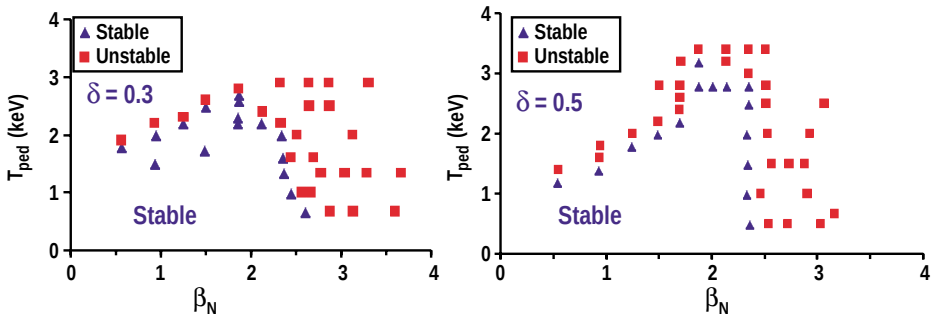


Fig. 6: Stability boundary in $T_{ped}$, $\beta_N$ space for the range $5 < n < 31$ for JET-like equilibria with $\kappa = 1.6$, (a) $\delta = 0.3$ (b) $\delta = 0.5$.

Strait *et al* [31] and Ferron *et al* [32], and several more recent papers by the DIII-D team, have employed the GATO [33] finite element ideal MHD code to study edge MHD stability and its relation to ELMs. It has consistently been found that giant ELMs are associated with low to intermediate $n$ instabilities with broad radial mode structures, while small ELMs are associated with more narrow unstable modes, often with higher $n$. Experiments on DIII-D have varied the plasma shape in order to change predicted pedestal stability limits and change expected ELM type, and have found good agreement between observations and MHD stability predictions [34, 35]. A "working model" of ELMs has been developed, as illustrated in Fig. 7 [34], using insight from experiment and $s - \alpha$ stability calculations, as well as toroidal stability calculations using GATO, ELITE, BALOO and BAL-MSC. Important features of the working model are that for "poor" shaping (i.e. low triangularity or very high squareness), there is no second stability access, and the pedestal $p'$ is limited by high $n$ (not infinite because of FLR stabilization) modes near the ideal ballooning $p'_c$. These high $n$ modes tend to have narrower radial mode structures and produce small high frequency ELMs. As the shape "improves", second stability access opens first at higher $n$ and then down to $n \sim 10$, and the most unstable mode is approximately the highest $n$ without second stability access. Edge $p'$ is then limited by intermediate-$n$ modes at values above the ballooning $p'_c$, and mode structures tend to be wider and produce large ELMs. Note that high collisionality, like poor shaping, has the same effect of cutting off second stability access, because it reduces the bootstrap current and increases $\hat{s}$.

A similar pedestal stability analysis has been carried out on JT-60U equilibria [36, 21], and it has been found that detailed stability analysis resolves apparent differences between JT-60U and DIII-D ELM behavior, and that wide mode structures are calculated for large JT-60U ELMs, and narrow mode structures for small "grassy" ELMs, just as in DIII-D. The narrow JT-60U mode structures in grassy ELM cases appear to be related to high edge $q$.

Saarelma *et al* [37, 38] have studied peeling-ballooning stability using ASDEX-U equilibria and the GATO code. Increasing bootstrap current is found to destabilize peeling modes, while stabilizing ballooning modes [37], supporting the ELM model of

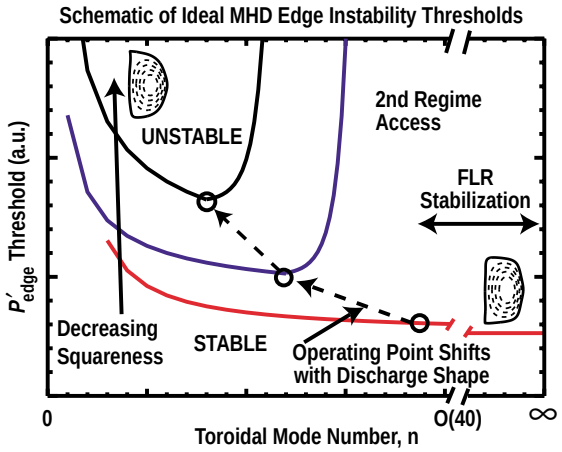


Fig. 7: Working model of ELMs in $p'$, $n$ space.

Connor *et al* [17]. Increasing triangularity stabilizes the peeling modes, while having little impact on the high $n$ ballooning limit, suggesting that low to intermediate-$n$ peeling modes may be responsible for ELMs in ASDEX-U. A recent study of type II ELMs in ASDEX-U [38] finds narrower $n = 3$ radial mode structures in small (type II) ELM cases than for large (type I) ELMs. The combination of high $\delta$ and high $q$ is responsible for the narrowing, and it is proposed that the narrow width contributes at least partially to the small ELM size. A model of the ELM cycle, extending that in [17], is also proposed to explain the dramatic difference in ELM energy loss between type I and type II ELMs (Fig. 8). Higher $j_a$ is needed to destabilize peeling modes at high $\delta$, high $q$, but the pressure gradient is similar because it is proposed to be limited by high-$n$ ballooning modes, whose stability boundary is insensitive to $\delta$ and $q$. Hence the ELM crash occurs in the type II case at higher current, closer to steady

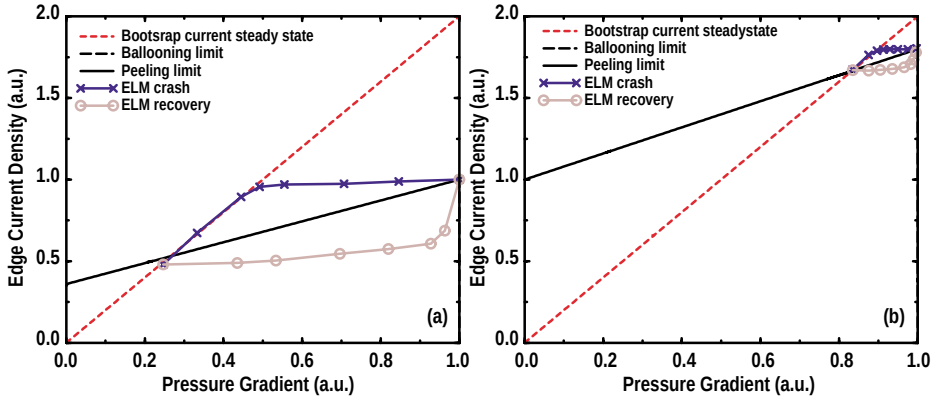


Fig. 8: (a) Type I and (b) Type II ELM cycle.

state bootstrap value for the given $p'$, and it is proposed that the current therefore decreases more quickly below the stability limit, leading to a smaller ELM.

Mossessian *et al* [13] studied the peeling-ballooning stability of EDA, ELM-free, and ELMy Alcator C-Mod discharges using the ELITE code. Intermediate $5 < n < 50$ growth rates were found to increase strongly with edge current, and to be higher with broader mode structure in ELMy cases than in EDA or ELM-free. Results appear consistent with a model of ELMs as intermediate-$n$ peeling-ballooning modes, while edge oscillation in EDA mode is due to resistive ballooning.

The above stability calculations on experimental equilibria have generally been carried out by by truncating the equilibria just inside the separatrix (to avoid numerical difficulties with mapping equilibria and/or with stability codes), and placing a vacuum outside. This truncation usually occurs in the vicinity of $\psi \gtrsim 0.99$ (MISHKA1,ELITE) or $\psi \sim 0.997$ (GATO), and in most cases it is found that the truncation point does not strongly affect stability calculations, though for peeling modes increasing the cutoff $\psi$ can in some cases be slightly stabilizing. A study has been carried out by Medvedev *et al* ([39] and references therein) to assess the impact of including the separatrix in MHD stability calculations, using the KINX code. Significant stabilization of kink modes was found in moving the boundary from $\psi = 0.95$ to $\psi = 1.0$ as expected.

### 3.2 Rotation and non-ideal MHD

The stabilizing effects of sheared toroidal rotation shear are well known in the context of high-$n$ ballooning modes (e.g. [40]) and resistive wall modes. Rotation is expected by many to have an important stabilizing impact on peeling-ballooning modes. Extensions to the ideal MHD model are also expected to have a significant quantitative impact on peeling mode stability calculations.

The diamagnetic drift ($\omega_*$) is considered a strong candidate to impact peeling-ballooning stability in the pedestal, because the strong pedestal pressure gradient leads to $\omega_*$ values that can exceed ideal MHD growth rates in many cases, particularly at higher $n$. The analytic relation [41, 42]

$$-\gamma_{MHD}^2 = \omega(\omega - \omega_{*i}) \quad , \tag{2}$$

where $\gamma_{MHD}$ is the ideal growth rate, implies that the ideal MHD instability becomes stabilized when $\omega_{*i}/2 > \gamma_{MHD}$. Eq. (2) neglects kinetic effects, and assumes a constant value for $\omega_{*i}$. Hastie, Catto and Ramos [43] have developed a formulation for treating the strong variation of $\omega_{*i}$ typical of the pedestal, and have found that strong variation of $\omega_{*i}$ diminishes its stabilizing effect.

Rogers and Drake [44] used nonlinear flux tube simulations of high $n$ ballooning modes using the Braginskii equations, and a simple analytic model, to demonstrate that $\omega_*$ effects significantly modify the ideal ballooning limit, and offered $\omega_*$ stabilization as an alternative to second stability to explain observations of $p' > p'_c$ in the

pedestal (a similar suggestion was made by Hahm and Diamond [45]). Comparisons with DIII-D data [12] indicate that the Rogers and Drake model does predict an approximate upper limit on $\alpha$ for the studied discharges, though it is more successful in predicting the behavior of discharges calculated to have second stability access in the pedestal, while it tends to over-predict $\alpha$ for discharges without second stability access. Extension of the model beyond $s - \alpha$ geometry may be useful for predicting such differences and the generally large shape dependence in the data.

Huysmans *et al* [46] have developed an extended version of the MISHKA code (MISHKA-D) which incorporates $\omega_*$ effects via a reduced version of the Mikhailovskii *et al* [47] extended MHD model. The strength of $\omega_{*i}$ stabilization is parameterized by $\tau$, the ratio of Alfvén to ion cyclotron frequency on axis. Calculations with MISHKA-D find eigenvalues in good agreement with Eq. (2) for the model equilibrium used. Stability boundaries for $n = 1$–$8$ peeling modes are shown in Fig. 9 [46]. The $\omega_*$ stabilizing effect is significant, and relatively independent of $n$ because both the growth rate and $\omega_{*i}$ increase linearly with $n$ in this regime. An equilibrium from a JET hot-ion H-mode is also studied. The edge current is found to be limited by $n = 2$ peeling modes, and $\omega_{*i}$ stabilization allows a 35% increase in stable $j_a$, while the edge pressure is limited by $n \sim 10$–$15$ ballooning modes around 30% above the ideal ballooning limit. Both peeling and ballooning stability limits have significant dependence on density, being more stable at low density.

The $\omega_{*i}$ stabilization models considered above do not take into account kinetic effects such as Landau damping and coupling to sound waves. Kinetic and gyrofluid calculations of ballooning modes, as well as two fluid analysis of FLR effects on internal kinks have found significant destabilizing effects which may to some extent counterbalance the stabilizing effects discussed above.

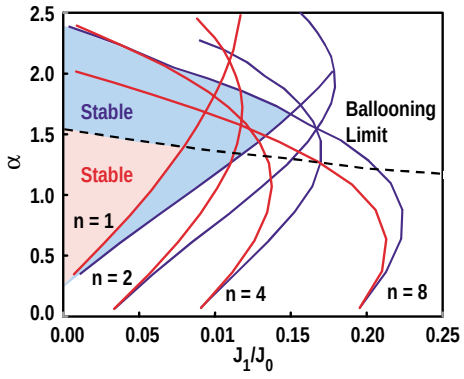


Fig. 9: Peeling mode stability limits in edge $\alpha$,$j_a$ for $1 < n < 8$, calculated without (thin lines) and with (thick lines) $\omega_{*i}$ stabilization, $\tau = 0.02$.

### 3.3 Nonlinear simulation and transport codes

The linear models discussed in the previous sections allow for prediction of limits on pedestal gradients, current, and even temperature, and also allow for the construction of semi-quantitative models of the ELM cycle. However, nonlinear, dynamic models will ultimately be needed for completely quantitative models of the ELM cycle and pedestal dynamics.

Nonlinear simulations have been undertaken with the BOUT [48] reduced Braginskii boundary turbulence code, which simulates a domain extending from the top of the pedestal, across the separatrix and into the scrape-off-layer (e.g. $0.95 < \psi < 1.05$). The kink term has recently been introduced into the BOUT formulation [21, 30], and current driven peeling modes have been observed and studied in the presence of $\omega_*$ and other two fluid effects. Achieving nonlinear saturation of the simulations in the presence of a strongly growing peeling mode has proved challenging.

An approach for modeling pedestal dynamics and the ELM cycle without undertaking challenging large scale nonlinear simulations, is to incorporate models of ELMs into existing transport codes, which evolve density, temperature and current profiles. While transport codes in the past have generally neglected the pedestal region, recent efforts have been made to extend their validity into the pedestal parameter regime. Janeschitz *et al* ([49] and references therein) have incorporated a model of turbulent transport suppression in the pedestal, and an ELM crash model based on ideal ballooning stability into the ASTRA transport code. Early simulations have found promising agreement with ASDEX-U and JET ELM cycles. Efforts are underway at several institutions to incorporate ELM models based on more detailed peeling-ballooning stability calculations into transport codes.

## 4 Summary

ELMs can limit tokamak performance both directly, via large transient heat loads to divertor plates, and indirectly, through constraints placed on the edge pedestal height which impact global confinement. Understanding the physics of ELMs has proved challenging, but such understanding is needed to reliably design Next Step fusion devices with both a high pedestal and tolerable ELMs.

The sharp pressure gradients in the H-mode transport barrier drive large bootstrap currents, and the combination of large $p'$ and $j$ provide drive for a variety of MHD instabilities over a wide range of toroidal mode numbers ($n$). We have reviewed a number of papers devoted to understanding the dual role played by the edge current, on the one hand driving peeling instabilities, while on the other hand reducing shear and providing second stability access to ballooning modes. The destabilizing coupling of peeling and ballooning modes has been discussed, and a series of papers studying pedestal MHD stability in shaped toroidal geometry have been reviewed, including discussions of new numerical tools such as the MISHKA and ELITE codes, which allow efficient computation of pedestal stability over a wide spectrum of $n$ values.

These comprehensive ideal MHD stability calculations have contributed to the development of a number of semi-quantitative models for the ELM cycle, and comparisons with experiment have yielded encouraging agreement with predictions of peeling or peeling-ballooning modes as ELM and "outer mode" triggering events. Understanding has reached the point where several efforts to control ELM behavior in tokamaks have been undertaken (e.g. [8, 50, 34]), and have yielded results in broad agreement with theoretical expectations. A significant limitation in theory/experiment comparisons has been the lack of direct measurements of the pedestal current. It is hoped that new diagnostic efforts (such as the lithium beam on DIII-D) will overcome this problem in the near future.

Several efforts to extend peeling and peeling-ballooning mode studies beyond the ideal MHD model have been discussed, and diamagnetic drift stabilization has been identified as an important factor in quantitative studies.

Ultimately, nonlinear studies using comprehensive physics models are needed to fully and quantitatively understand ELM and pedestal dynamics. We have described early efforts to include peeling modes in the Braginskii-based boundary turbulence code BOUT, and efforts to incorporate models of ELMs and pedestal microturbulence suppression into transport codes. Transport codes including ELM models have successfully modeled several aspects of the ELM cycle, and appear to be a promising tool for near term progress.

## Acknowledgements

This work was funded by the U.S. Department of Energy under grant No. DE-FG03-95ER54309, and by the UK Dept. of Trade and Industry and Euratom. The authors gratefully acknowledge assistance from Drs. X.Q. Xu, G.T.A. Huysmans, S. Saarelma, D. Mossessian, L.L. Lao, T.H. Osborne, J.R. Ferron, R.J. Groebner, and A.D. Turnbull in assembling this manuscript.

## References


[1] Zohm, H., Plasma Phys. Contol. Fusion **38** (1996) 105
[2] Connor, J.W., Plasma Phys. Control. Fusion **40** (1998) 191
[3] Suttrop, W., Plasma Phys. Contol. Fusion **42** (2000) A1
[4] Lao, L.L., Plasma Phys. Control. Fusion **42** (2000) A51
[5] Hubbard, A.E., Plasma Phys. Control. Fusion **42** (2000) A15
[6] Hatae T.,*et al*, Nucl. Fusion **41** (2001) 285
[7] Doyle, E.J., *et al*, Phys. Fluids B **3** (1991) 2300
[8] Nave, M.F.F., *et al*, Nucl. Fusion **39** (1999) 1567
[9] Takase, Y., *et al*, Plasma Phys. Control. Nucl. Fusion Research 1996 Vol. 1 p. 475, IAEA, Vienna (1997)
[10] Greenwald, M., *et al*, Phys. Plasmas **6** (1999) 1943
[11] Burrell, K.H., *et al*, Phys. Plasmas **8** (2001) 2153
[12] Osborne, T.H., *et al*, Plasma Phys. Control. Fusion **42** (2000) A175
[13] Mossessian, D., *et al*, EPS Conf. Plasma Phys. Control. Fusion (2001)
[14] Frieman, E.A., *et al*, Phys. Fluids **16** (1972) 1108
[15] Lortz, D., Nucl. Fusion **15** (1975) 49
[16] Wesson, J.A., Nucl. Fusion **18** (1978) 87
[17] Connor, J.W., *et al*, Phys. Plasmas **5** (1998) 2687
[18] Hegna, C.C., *et al*, Phys. Plasmas **3** (1996) 584
[19] Wilson, H.R., *et al*, Phys. Plasmas **6** (1999) 1925
[20] Wilson, H.R., and Miller, R.L., Phys. Plasmas **6** (1999) 873
[21] Snyder, P.B., *et al*, EPS Conf. Plasma Phys. Control. Fusion (2000)
[22] Wilson, H.R., *et al*, EPS Conf. Plasma Phys. Control. Fusion (2001)
[23] Ramos, J.J., *et al*, Phys. Plasmas **8** (2001) 2029
[24] Turnbull, A.D., *et al*, J. Comp. Phys. **66** (1986) 391
[25] Manickam, J., Phys. Fluids B **4** (1992) 1901
[26] Huysmans, G.T.A., *et al*, EPS Conf. Plasma Phys. Control. Fusion (1995)
[27] Huysmans, G.T.A., *et al*, Nucl. Fusion **38** (1998) 179
[28] Huysmans, G.T.A., *et al*, Nucl. Fusion **39** (1999) 1489
[29] Mikailovskii, A.B., *et al*, Plasma Phys. Rep. **23** (1997) 844
[30] Snyder, P.B., *et al*, Bull. Am. Phys. Soc. **45** (2000) 277
[31] Strait, E.J., *et al*, EPS Conf. Plasma Phys. Control. Fusion (Lisbon, Portugal) Vol 17C Part 1 (1993) p 211
[32] Ferron, J.R., *et al*, EPS Conf. Plasma Phys. Control. Fusion (1995)
[33] Bernard, L.C., *et al*, Comp. Phys. Commun. **24** (1981) 377
[34] Ferron, J.R., *et al*, Phys. Plasmas **7** (2000) 1976
[35] Osborne, T.H., *et al*, EPS Conf. Plasma Phys. Control. Fusion (1997)
[36] Lao, L.L., *et al*, Nucl. Fusion **41** (2001) 295
[37] Saarelma, S., *et al*, Plasma Phys. Control. Fusion **42** (2000) A139
[38] Saarelma, S., *et al*, EPS Conf. Plasma Phys. Control. Fusion (2001)
[39] Medvedev, S.Yu., *et al*, EPS Conf. Plasma Phys. Control. Fusion (2001)
[40] Miller, R.L., *et al*, Phys. Plasmas **2** (1995) 3676
[41] Roberts, K.V., Taylor, J.B., Phys. Rev. Lett. **8** (1962) 197
[42] Tang, W.M., *et al*, Nucl. Fusion **22** (1982) 1079
[43] Hastie, *et al*, Phys. Plasmas **7** (2000) 4561
[44] Rogers, B.N., Drake, J.F., Phys. Plasmas **6** (1999) 2797
[45] Hahm, T.S., Diamond, P.H., Phys. Fluids **30** (1987) 133

[46] Huysmans, G.T.A., *et al*, "Modeling of Diamagnetic Stabilization of Ideal MHD Instabilities associated with the Transport Barrier." to appear in Phys. Plasmas (2001)
[47] Mikhailovskii, A.B., *et al*, Plasma Phys. Rep. **23** (1997) 844
[48] Xu, X., *et al*, Nucl. Fusion **40** (2000) 731
[49] Janeschitz, G., *et al*, EPS Conf. Plasma Phys. Control. Fusion (2001)
[50] Fielding, S.J., *et al*, EPS Conf. Plasma Phys. Control. Fusion (2001)

Received October 15, 2002.